Composites Science and Technology 276 (2026) 111517

Contents lists available at ScienceDirect

Composites Science and Technology

journal homepage: www.elsevier.com/locate/compscitech

Geometric scaling of reinforcement and its pivotal role in design of 3D woven composites

Elena Sitnikova [a,*], Shuguang Li [b]

[a] Department of Mechanical Engineering, School of Engineering, University of Southampton, Southampton, SO17 1BJ, UK
[b] Faculty of Engineering, The University of Nottingham, Nottingham, NG8 1BB, UK

ARTICLE INFO

Handling Editor: Marino Quaresimin

Keywords:
3D woven composites
Layer-to-layer angle interlock
Elastic properties
Computational characterisation
Geometric scaling
Design method
Designable parameters

ABSTRACT

Geometric scaling has been defined as means of producing equivalent 3D layer-to-layer angle interlock woven composite configurations that have different reinforcement geometries but identical, or very similar, effective elastic properties. Scaling rules have been derived under condition that the key geometric properties of the weave: the interlocking angle, global fibre volume fraction and weft to warp tow volume ratio, should not be affected by scaling. The role of tow sizes as designable parameters directly associated with scaling has been established for the first time. With scaling method in place, design of 3D woven composites can be defined as a two-stage process, where the effective elastic properties are varied via systematic variation of tow densities, while scaling is applied at a post-processing stage to ensure the practicality of design. The design process is comprehensive in a sense that it involves all the designable parameters, explicitly defining their roles and contribution.

1. Introduction

Vast variety of internal constructions of 3D woven composites offers exceptional opportunities for tailoring their material properties to facilitate their efficient applications. As in all types of composites, the structure of reinforcement can have a profound influence on their mechanical behaviour, and substantial experimental evidence to it was accumulated over the past few decades [1–5]. To take advantage of variety of achievable mechanical responses, a methodology must be in place relating the structural parameters of 3D woven reinforcements to the mechanical behaviour of composites. This would inform the designer how to modify the reinforcement in a way that would deliver the desired performance.

Until recently, research into 3D woven composites was largely focused on development and application of computational models for their characterisation [6,7]. As understanding that behaviour of these materials can and should be controlled through design started to emerge, attempts were being made to systematically associate features of 3D woven architecture with the mechanical behaviour. Via direct application of material characterisation models, parametric studies were devised for capturing the trends in variation of the effective properties relative to some of the parameters of woven reinforcement. Specifically, parametric study showing the influence of tow densities on variation of the in-plane Young's moduli and strengths in 3D angle interlock woven composites was reported in Ref. [8], while correlation between tow cross-section size and effective elastic properties was examined in Ref. [9].

While such parametric studies can help to expose general trends in variation of the effective properties, thus informing the process of material selection, the optimisation as a problem-specific method of design is meant to provide a definitive solution. In application to design of woven composites, the optimisation is typically formulated as a mathematical problem with the objective of maximising or minimising certain effective properties [10,11]. Such optimisations employ analytical methods of material characterisation due to their high computational efficiency and relative ease of implementation compared to characterisation relying of use of finite element (FE) method.

Most recently, wide availability of artificial intelligence (AI) methods and tools further boosted the development of design approaches. They offer a way of incorporating the FE-based material characterisation into the design problems. Methods such as artificial neural networks (ANN) are employed, where the training data are generated using the finite element material characterisation models. The inputs of such ANN-based characterisation procedures can be effective

* Corresponding author.
E-mail address: elena.sitnikova@soton.ac.uk (E. Sitnikova).

https://doi.org/10.1016/j.compscitech.2026.111517
Received 22 July 2025; Received in revised form 17 December 2025; Accepted 2 January 2026
Available online 7 January 2026

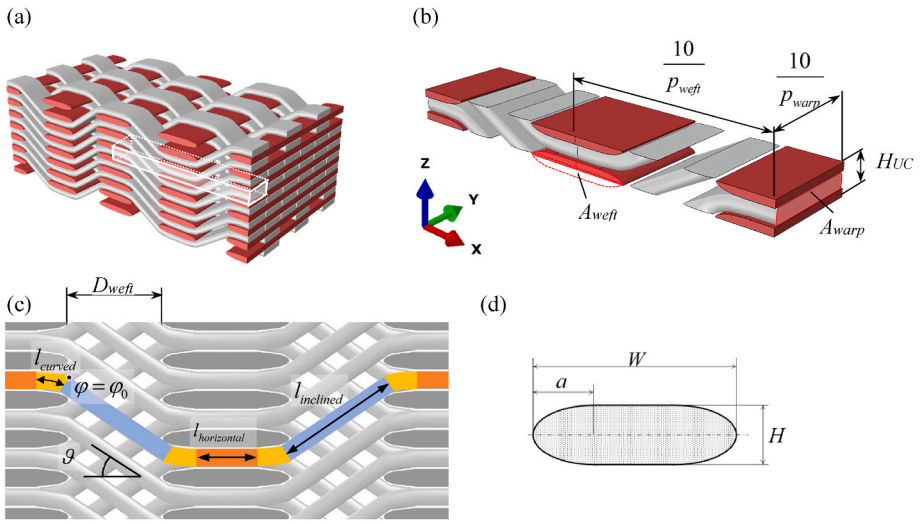

Fig. 1. Parametrisation of woven composite: (a) woven architecture; (b) unit cell with the controllable properties and parameters specified; (c) geometric properties and parameters of the weave (d) parametrisation of the tow cross-section.

properties of the constituents [12], often in combination with geometric dimensions of woven reinforcements [13–15]. While the process of training the neural networks is usually computationally demanding, once created, the application of the method does not require significant computing resources [16], thus offering a computationally efficient means of material characterisation. The main outcome of such computational exercises that is typically reported is the close agreement between predictions obtained using the ANN-based characterisation and the data obtained via conventional computational [13,15] or experimental [14] characterisation. Once established, the ANN-based characterisation can be incorporated in optimisation problem, as was done in Ref. [15] where maximising the effective elastic modulus and strength were set as an objective of optimisation.

Despite the apparent interest and certain progress in development of design methods, their practicality and effectiveness remain questionable, because two major issues are recurring in formulation of the design problems: definition of designable parameters and a formulation of the design method itself. Often, geometric dimensions of the weave are treated as the designable parameters [10,11]. The use of geometric parameters, such as the height and the width of the tows, has been a commonplace practice in material characterisation exercises, but these parameters are not truly designable in a sense that many combinations of such parameters are simply not practical. Furthermore, due to high variability of the internal woven architecture, they can only be defined in a statistical sense. A more appropriate alternative is to use the parameters associated with the manufacturing (weaving and forming) processes as the designable ones directly. The geometric parameters, that are usually required for reproducing the woven architecture in the models are calculated from the manufacturing ones [17,18]. Direct use of manufacturing parameters in design facilitates communication with the manufacturer and allows to naturally incorporate the manufacturing restrictions in the design. Even then, the number of such parameters is still too large to comprehensively analyse and document their influence on the effective properties of the material. Because of that, studies of this kind are often restricted to certain groups of parameters, such as tow densities in Refs. [3,8]. Use of woven topologies alone as means of varying the mechanical performance is yet another design consideration that was brought up in Ref. [19].

Formulation and implementation of design method is another major issue. Given that the proposed design methods involve only some of the parameters associated with structure of 3D woven reinforcement, often chosen based on intuition, such methods are not sufficiently comprehensive. They are also demanding in terms of implementation and are not sufficiently robust to be readily applied by the users.

Addressing the issue of lack of design tools for 3D woven composites, the authors established a drastically different approach to design which is free from the drawbacks as described above. At the heart of it is use of the key properties of the weave (KPoWs) as were defined in Ref. [20]. These are the global fibre volume fraction, the interlocking angle, defined as the slope of the inclined part of the warp tow [21] and the ratio of the weft to the warp tow volumes, referred to for brevity as the 'tow ratio'. The KPoWs are geometric characteristics that represent combined contribution of designable (manufacturing-related) parameters as were defined in Ref. [20]. Unlike designable parameters, they can be directly related to the effective properties, because effective properties follow distinctive variation trends relative to KPoWs, as was demonstrated in Ref. [21]. Furthermore, proper use of the KPoW allowed to define permissible variations of manufacturing parameters, so that they would deliver only valid 3D woven architectures.

The identification and the subsequent use of trends in variation of mechanical properties to achieve a desired mechanical behaviour is a conventional path to take in design. However, when designing the advanced materials such as 3D woven composites, an equally important question to ask is whether there exists equivalence of woven architectures, where composites of substantially different internal geometry would deliver similar mechanical behaviour. This is a conceptually new consideration in design of the advanced materials having highly intricate internal architectures that has not been addressed to date. Identifying such variations would have profound implications on the design procedures. The present paper is to establish the method for defining the equivalent configurations and to explain their implications on design of 3D woven composites.

2. Design scheme for 3D woven layer-to-layer angle interlock composites

The method of defining equivalent configurations of 3D woven composites will be derived as an extension of design method based on use of KPoWs as was established in Ref. [20]. To facilitate referencing and explanations, brief summary of the method is given in this section. The type of 3D woven reinforcement under consideration is layer-to-layer angle interlock one, typical architecture of which is shown in Fig. 1(a). As has been argued in Ref. [22], from considerations of mechanics, this structure of reinforcement should be able to offer better performance under the lateral loading than those in which the tows are aligned with the transverse direction.

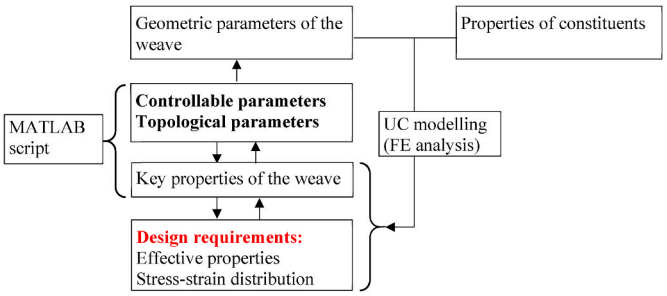

Fig. 2. Relationships between groups of properties and parameters involved is woven composites design.

2.1. Parametrisation of 3D woven composites

Proper parametrisation of 3D woven reinforcement is imperative for formulation of the design methodology. It included three consecutive steps as follows:

1) Parametrisation of the geometry and topology of the woven reinforcement, through which definition of large variety of woven reinforcements has been unified [21]. The main use of this parametrisation is to facilitate generating the unit cell models in the FE solver, using which the material characterisations are carried out.
2) Expressing the geometric parameters in terms of the manufacturing parameters, as has been accomplished in Ref. [22], where the latter have been referred to as controllable parameters. Controllable parameters ensure the design feasibility in a sense that they equip the manufacturers and the designers with common terminology. Equally important consideration is that they help to eliminate the subjectivity from definition of the geometric parameters, replacing their direct measurement that can be rather subjective.
3) Derivation of the KPoWs [20] which makes the design practical by allowing to establish the association between the controllable parameters and the effective properties of composite.

Relationships between different types of parametrisations and their application in design exercises are shown schematically in Fig. 2.

Controllable parameters are marked on the unit cell model in Fig. 1 (b). Two of these parameters, p_{weft} and p_{warp}, are the weft and the warp tow densities, respectively. These are conventional weaving parameters indicating the number of respective tows in 10 mm of the woven fabric. Parameter H_{UC} denotes the height of the unit cell, and for unit cell parametrised following [21], it is defined as

$$H_{UC} = H_{warp} + H_{weft}, \tag{1}$$

where H_{weft} and H_{warp} are the heights of the weft and the warp tow cross-sections, respectively. Parameters H_{UC} is directly related to the thickness of the preform, which is yet another manufacturing parameter. It has been established in Ref. [20] that H_{UC} also represents the density of the packing of the tows in the weave but in the thickness direction: the more unit cells are accommodated within the given thickness of the composite panel, the denser the through-the-thickness packing of the tows. For ease of referencing, H_{UC} been referred to as through-the-thickness tow density. The weft and the warp tow cross-sectional areas, A_{weft} and A_{warp}, respectively, represent the joint contribution of the controllable parameters associated with the tows. Their explicit expressions are

$$A_{weft} = \frac{\pi d_{f,weft}^2 N_{weft}}{4V_{f,weft}} \quad \text{and} \quad A_{warp} = \frac{\pi d_{f,warp}^2 N_{warp}}{4V_{f,warp}}, \tag{2}$$

where d_f is a filament diameter, N is the number of the filaments in the tow, V_f is the intra-tow fibre volume fraction, and subscripts 'weft' and 'warp' refer to parameters associated with the weft and the warp tows, respectively. Tow cross-sectional areas have been referred to as the controllable properties in Ref. [20] to differentiate them from individual controllable parameters. Note that tow cross-sectional areas are not used directly by the weavers as designable parameters when producing preforms, however, according to Eq. (2), the size of cross-section area is effectively defined by the filament diameter and filament count, both of which are designable characteristics of the tows. This justifies treating of the cross-sectional areas as designable properties, as is further elaborated in Ref. [20].

To fully define the woven architecture, in addition to three controllable parameters and two controllable properties, the topological parameters should be specified. These are the integer parameters that define the path of the warp tows within the weave and their arrangement in the weave relative to each other. Complete account on definition of the topological parameters is given in Ref. [21] and their role in design exercises was elaborated in Ref. [20]. Note that in the present paper, the discussion will concentrate around the geometric characteristics of the weave and not the topological ones, because unlike the geometry, the topology of the weave is not scalable.

Parameters of tow cross-section are marked in Fig. 1(d), that shows a sketch of a cross-section idealised as a rectangle with two semi-ellipses on the sides. These parameters are the height, H, the width, W, and the measure of roundness, $\gamma \in (0,1]$, expressed as

$$\gamma = \frac{2a}{W}, \tag{3}$$

where a is the length of the horizontal semi-axis of the elliptical part of the cross-section, also marked in Fig. 1(d). One more geometric parameter, the distance between the weft tows, denoted as D_{weft}, is marked in Fig. 1(c). The geometric parameters have been expressed explicitly in terms of controllable parameters in Ref. [20] as follows:

$$W_{warp} = \frac{10}{p_{warp}}, \tag{4}$$

$$H_{warp} = \frac{A_{warp} p_{warp}}{10\Gamma_{warp}}, \tag{5}$$

$$H_{weft} = H_{UC} - H_{warp} = H_{UC} - \frac{p_{warp} A_{warp}}{10\Gamma_{warp}}, \tag{6}$$

$$W_{weft} = \frac{10\Gamma_{warp} A_{weft}}{\left(10\Gamma_{warp} H_{UC} - A_{warp} p_{warp}\right)\Gamma_{weft}}, \tag{7}$$

and

$$D_{weft} = \frac{10}{p_{weft}} - \frac{10\Gamma_{warp} A_{weft}}{\left(10\Gamma_{warp} H_{UC} - A_{warp} p_{warp}\right)\Gamma_{weft}}, \tag{8}$$

where

$$\Gamma_{warp} = \gamma_{warp}\left(\frac{\pi}{4} - 1\right) + 1, \quad \Gamma_{weft} = \gamma_{weft}\left(\frac{\pi}{4} - 1\right) + 1. \tag{9}$$

Expressions (4)–(8) explicitly relate the geometric parameters to the controllable ones. Using them, any given set of controllable parameters can be converted to the geometric ones, based on which geometry of the UC can be generated in the FE solver. Note that parameters γ_{weft} and γ_{warp} have not been expressed in terms of the controllable ones; furthermore, they are involved explicitly in expressions (4)–(8). The reason for doing so will be given once the nature of these parameters will be explained in subsection 4.1. Also note that Eqs. (4)–(8) are unit-dependent in a sense that they were derived for tow densities defined as the number of tows in 1 cm of fabric hence factor of 10 in all the derived expressions. These equations give geometric dimensions in mm, but the units can be changed in a straightforward way, if desired.

The KPoWs have been explicitly derived as functions of geometric

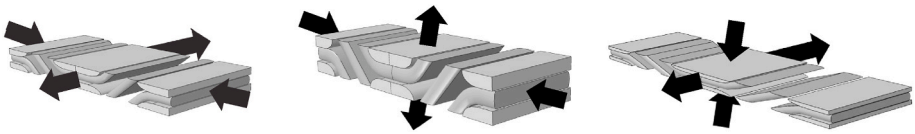

Fig. 3. Tow density variation schemes: (a) H_{UC} is kept constant (scheme 1); (b) p_{warp} is kept constant (scheme 2) and (c) p_{weft} is kept constant (scheme 3).

and controllable parameters. The interlocking angle, marked as ϑ in Fig. 1(c), has been determined as [20]

$$\tan\vartheta = \frac{H_{weft}}{W_{weft}\gamma_{weft}}\cot\varphi_0, \tag{10}$$

where φ_0 is the parameter in the parametric equation of the elliptical part of the weft cross-section profile at which the warp tow becomes straight, as marked in Fig. 1(c). It is determined from a transcendental equation for φ as [20]

$$\begin{aligned} &-(n_{steep}-1)\left(\frac{H_{warp}}{H_{weft}}+1\right)\sin\varphi+\left(\frac{D_{weft}}{W_{weft}\gamma_{weft}}+1\right)\cos\varphi \\ &-\frac{H_{warp}}{H_{weft}}\sqrt{\sin^2\varphi+\left(\frac{H_{weft}}{W_{weft}\gamma_{weft}}\right)^2\cos^2\varphi-1}=0 \end{aligned} \tag{11}$$

through Newton's iterations. This function is defined within a range $\varphi\in\left(0,\frac{\pi}{2}\right)$ and it is monotonic over this range, therefore, for a given set of geometric parameters it always has a unique solution.

The global fibre volume fraction has been expressed as follows [20]:

$$V_{f,global}=\frac{A_{weft}p_{weft}}{10H_{UC}}V_{f,weft}+\frac{A_{warp}p_{warp}}{10H_{UC}}kV_{f,warp} \tag{12}$$

and the tow ratio expression is

$$\frac{V_{weft}}{V_{warp}}=\frac{A_{weft}p_{weft}}{A_{warp}p_{warp}k}. \tag{13}$$

The non-dimensional property k in Eqs. (12) and (13) has been derived as:

$$k=\frac{p_{weft}}{10n_{skip}}(l_{horizontal}+l_{inclined}+2l_{curved}). \tag{14}$$

where $l_{horizontal}$ and $l_{inclined}$ are the lengths and l_{curved} is the arc length of warp tow segments highlighted in Fig. 1(c). Their explicit expressions are [20]

$$l_{horizontal}=n_{skip}\left(W_{weft}+D_{weft}\right)-W_{weft}\gamma_{weft}-D_{weft}\,, \tag{15}$$

$$l_{inclined}=\sqrt{\begin{aligned}&\left(\left(W_{weft}\gamma_{weft}+\frac{H_{warp}H_{weft}}{r}\right)\cos(\varphi_0)-W_{weft}\gamma_{weft}-D_{weft}\right)^2\\&+\left(\left(H_{weft}+\frac{H_{warp}W_{weft}\gamma_{weft}}{r}\right)\sin(\varphi_0)+(n_{steep}-1)\left(H_{warp}+H_{weft}\right)\right)^2\end{aligned}} \tag{16}$$

and

$$\begin{aligned} l_{curved}=&\frac{H_{warp}}{2}\left(\frac{\pi}{2}-\arctan\left(\frac{W_{weft}\gamma_{weft}}{H_{weft}}\tan\varphi_0\right)\right)\\&+\frac{H_{weft}}{2}\left(\int_0^{\frac{\pi}{2}}\sqrt{1-m\sin^2\varphi}\,d\varphi-\int_0^{\varphi_0}\sqrt{1-m\sin^2\varphi}\,d\varphi\right), \end{aligned} \tag{17}$$

where

Table 1
Reference tow density combinations corresponding to three variation schemes and the benchmark configuration from [20].

	p_{weft}, cm^{-1}	p_{warp}, cm^{-1}	H_{UC}, mm
Benchmark	2.4	7	0.41
Scheme1	1.5	8	0.41
	4.1	5	0.41
	5	4	0.41
Scheme 2	1.6	7	0.37
	3.6	7	0.48
	5	7	0.58
Scheme 3	2.4	8	0.46
	2.4	5	0.32
	2.4	4	0.28

$$m=1-\left(\frac{W_{weft}\gamma_{weft}}{H_{weft}}\right)^2 \text{ and}$$
$$r=W_{weft}\gamma_{weft}\sqrt{\sin^2(\varphi_0)+\left(\frac{H_{weft}}{W_{weft}\gamma_{weft}}\right)^2\cos^2(\varphi_0)}. \tag{18}$$

Note that the choice of geometric or controllable parameters in expressions of KPoWs was dictated only by convenience of presentation. Obviously, the geometric parameters in the expressions of KPoWs can always be replaced by their expressions in terms of controllable parameters as given by Eqs. (4)–(8), but the drawback of such exercise is that it would produce excessively bulky equations.

Having been explicitly derived, the expressions of the KPoWs have been implemented as a Matlab script [23]. The special significance of KPoWs in design is that the effective elastic properties follow distinctive variation trends with KPoWs, in view of which the design exercise can be reduced to a large extent to variation of KPoWs using the Matlab script.

2.2. Valid variations of controllable parameters

The variation of controllable parameters cannot be arbitrary. Random selection of controllable parameters can easily result in non-practical composite configurations that have unreasonably high or low global fibre volume fractions. The solution to this issue offered in Ref. [20] was to consider the variations of controllable parameters systematically, following what has been referred to as the tow density variation schemes.

Valid variations of tow densities were defined as such that maintain the global fibre volume fraction at a designated practical value, denoted as the 'guideline ceiling'. Note that the use of global volume fraction as a design constraint has also been adopted in Ref. [15]. To produce a valid configuration from a benchmark one, two tow densities should be varied simultaneously, with their variation following the opposite tendencies: if change in one causes tightening of the weave, the other should 'loosen' it enough to keep the global fibre volume fraction constant. Three possible tow density variation types are illustrated in Fig. 3. In Table 1, values of tow densities associated with each scheme are given explicitly, three sets for each scheme, along with the 'Benchmark' tow density values, relative to which variation schemes were defined. This benchmark configuration was used merely to facilitate the explanation, and the design procedures and discussion in Ref. [20] would remain valid irrespective of the choice of the benchmark configuration. Ten composite configurations defined by tow density combinations from Table 1

will be collectively referred to as the 'Reference' configurations. These tow density combinations have been previously determined in Ref. [20] under condition that the global fibre volume fraction of the composite was kept constant at $V_{f,global} = 0.55$. All the configurations had identical topologies as that correspond to the values of topological parameters $n_{step} = n_{skip} = 1$, $n_{steep} = n_{deep} = 2$ as were defined in parametrisation [21]. The variation schemes were established while keeping the parameters associated with the tows as in Eq. (2) constant at $d_{f,warp} = d_{f,weft} = 5$ μm, $N_{warp} = N_{weft} = 12$ K, $\gamma_{warp} = 0.05$ and $\gamma_{weft} = 0.5$.

3. Equivalent weave configurations

For each tow density variation scheme, the variation of KPoWs follows distinctive trends, as was established in Ref. [20]. However, there are two controllable properties, namely, the cross-sectional areas of the weft and warp tows, that also explicitly involved in definition of KPoWs and whose variation will also affect the KPoWs. For design method to be comprehensive, the nature of the association between the KPoWs and the cross-sectional areas must be understood so it could be efficiently utilised in the design exercises. This will be achieved in the present section.

3.1. Expressing KPoWs in non-dimensional terms

Considering transcendental equation (11), it is easy to see that it is non-dimensional since all its terms are non-dimensional. Denoting them as

$$B = \frac{H_{warp}}{H_{weft}}, C = \frac{H_{weft}}{W_{weft}\gamma_{weft}} \text{ and } Q = \frac{D_{weft}}{W_{weft}\gamma_{weft}} \tag{19}$$

allows re-writing Eq. (11) and the expression for interlocking angle (10) simply as

$$(Q+1)\cos\varphi - B\sqrt{\sin^2\varphi + C^2\cos^2\varphi} - (n_{steep}-1)(B+1)\sin\varphi - 1 = 0 \tag{20}$$

and

$$\tan\vartheta = C\cot\varphi_0, \tag{21}$$

respectively. It can be shown explicitly that the two remaining KPoWs, namely, the tow ratio (13) and the global fibre volume fraction (12), can also be written as functions of as B, C and Q. This is achieved through simple algebraic manipulations of their original expressions that primarily include re-arrangement of the terms in Eqs. (12)–(18). For completeness of presentation, the detailed derivations are provided as Supplementary Material, while the final expressions of the tow ratio and the global fibre volume fraction are as follows:

$$\frac{V_{weft}}{V_{warp}} = \frac{A_{weft}p_{weft}}{A_{warp}p_{warp}k} = \frac{\Gamma_{weft}}{\Gamma_{warp}B\left(Q\gamma_{weft}+1\right)k} \tag{22}$$

and

$$V_{f,global} = \frac{1}{1+B}\left(\frac{\Gamma_{weft}}{\left(Q\gamma_{weft}+1\right)}V_{f,weft} + \Gamma_{warp}BkV_{f,warp}\right), \tag{23}$$

respectively. The new expression of property k (14) is

$$k = \frac{\gamma_{weft}}{n_{skip}\left(Q\gamma_{weft}+1\right)}(l_h + l_i + 2l_c). \tag{24}$$

Note that the terms in brackets no longer exactly define the lengths of different warp top segments marked in Fig. 1(c), but represent their non-dimensional counterparts hence different notations. Their expressions have been derived as

$$l_h = \left(\frac{n_{skip}}{\gamma_{weft}} - 1 + (n_{skip}-1)Q\right) \tag{25}$$

$$l_i = \sqrt{\left(\left(1+\frac{C^2B}{r_{nd}}\right)\cos\varphi_0 - 1 - E\right)^2 + C^2\left(\left(1+\frac{B}{r_{nd}}\right)\sin\varphi_0 + (n_{steep}-1)(B+1)\right)^2}, \tag{26}$$

$$l_c = \frac{C}{2}\left[B\left(\frac{\pi}{2} - \arctan\left(\frac{1}{C}\tan\varphi_0\right)\right) + \left(\int_0^{\frac{\pi}{2}}\sqrt{1-m\sin^2\varphi}\,d\varphi - \int_0^{\varphi_0}\sqrt{1-m\sin^2\varphi}\,d\varphi\right)\right] \tag{27}$$

where

$$r_{nd} = \sqrt{\sin^2\varphi_0 + C^2\cos^2\varphi_0} \text{ and } m = 1 - \left(\frac{1}{C}\right)^2. \tag{28}$$

To verify these derivations, all these equations have been implemented as a MATLAB script [24] that was then used to calculate the KPoWs at different combinations of controllable parameters. There results were compared with those calculated using Eqs. (11)–(18), that have been extensively verified previously in Ref. [20]. Exact match was obtained between the two in all cases.

3.2. Scaling rule in a general case

As was argued in Ref. [20], valid variations of tow densities should be such that retain the same global fibre volume fraction $V_{f,global}$. Same constraint should apply to variation of the controllable properties A_{weft} and A_{warp}. Given that $V_{f,global}$ (23) is fully defined by B, C and Q, constancy of $V_{f,global}$ can be achieved if none of B, C and Q is affected by variation of the A_{weft} and A_{warp}. As a by-product, this will also ensure constancy of the other two KPoWs, since they are also fully defined as functions of B, C and Q.

In the most general case, the weft and the warp tow cross-sectional areas can be scaled as

$$A^s_{weft} = s_1A_{weft} \text{ and } A^s_{warp} = s_2A_{warp}, \tag{29}$$

respectively, where s_1 and s_2 are the scaling factors, and the subscript 's' henceforth designates a scaled value of a controllable parameter or property.

As a direct consequence of changing the size of the tows, tightening or loosening of the weave will occur. To compensate for it and retain the

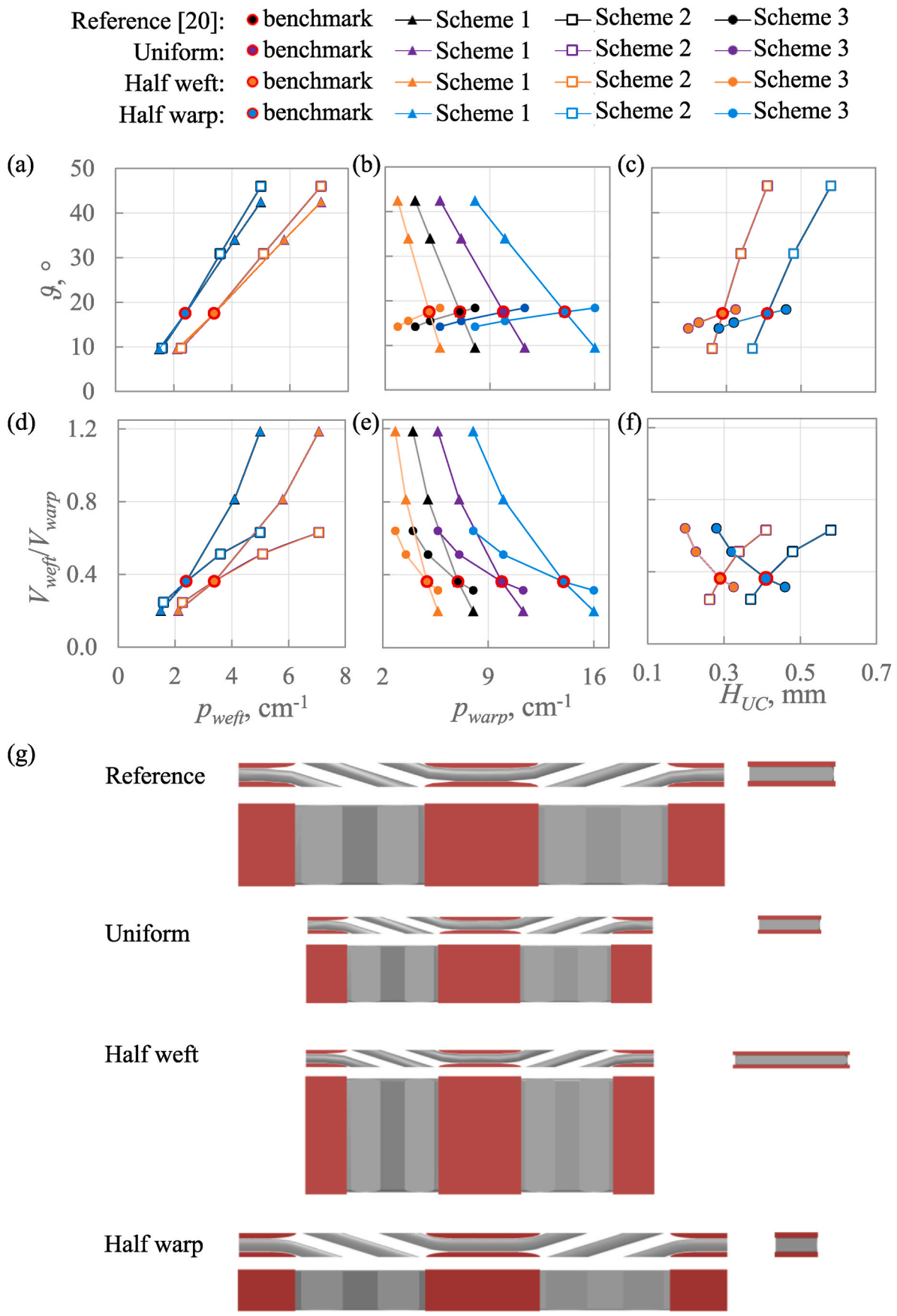

Fig. 4. Interlocking angle and the tow ratio as functions of the weft tow density (plots (a) and (d), respectively), weft tow density (plots (b) and (e)) and H_{UC} (plots (c) and (f)). Plot (g) - geometries of four benchmark UCs configurations that have equivalent KPoWs.

same global fibre volume fraction, the tow densities p_{warp}, p_{weft} and H_{UC} are allowed to vary according to

$$p^s_{warp} = s_{warp}p_{warp}, \quad p^s_{weft} = s_{weft}p_{weft} \quad \text{and} \quad H^s_{UC} = s_H H_{UC}, \tag{30}$$

where s_{warp}, s_{weft} and s_H are their respective scaling factors.

Making use of Eqs. (4)–(8) that relate the geometric parameters to controllable ones, B, C and Q can be expressed in terms of controllable parameters as

$$B = \frac{H_{warp}}{H_{weft}} = \frac{A_{warp}p_{warp}}{10\Gamma_{warp}H_{UC} - A_{warp}p_{warp}}, \tag{31}$$

$$C = \frac{H_{weft}}{W_{weft}\gamma_{weft}} = \left(\frac{10\Gamma_{warp}H_{UC} - A_{warp}p_{warp}}{10\Gamma_{warp}}\right)^2 \frac{\Gamma_{weft}}{A_{weft}}, \tag{32}$$

$$Q = \frac{D_{weft}}{W_{weft}\gamma_{weft}} = \left(\frac{\Gamma_{weft}}{\Gamma_{warp}} \frac{\left(10\Gamma_{warp}H_{UC} - A_{warp}p_{warp}\right)}{A_{weft}p_{weft}} - 1\right) \frac{1}{\gamma_{weft}}. \tag{33}$$

Replacing controllable parameters and properties in the expression of term B (31) with their scaled counterparts (29)–(30) yields

$$B^s = \frac{s_2 A_{warp}s_{warp}p_{warp}}{10\Gamma_{warp}s_H H_{UC} - s_2 A_{warp}s_{warp}p_{warp}} = \frac{A_{warp}p_{warp}}{10\Gamma_{warp}\frac{s_H}{s_2 s_{warp}}H_{UC} - A_{warp}p_{warp}} \tag{34}$$

Comparing it with the original expression of B given by Eq. (31), it is easy to see that scaling introduced factor $s_H/(s_2 s_{warp})$. Therefore, setting

$$\frac{s_H}{s_2 s_{warp}} = 1 \tag{35}$$

will ensure that $B^s = B$. This produces a constraint on scaling coefficients as follows:

$$s_H = s_{warp}s_2. \tag{36}$$

Next, scaling term C, after some basic algebraic manipulations involving Eq. (36), one obtains

$$\begin{aligned} C^s &= \left(\frac{10\Gamma_{warp}s_H H_{UC} - s_2 A_{warp}s_{warp}p_{warp}}{10\Gamma_{warp}}\right)^2 \frac{\Gamma_{weft}}{s_1 A_{weft}} \\ &= \frac{(s_2 s_{warp})^2}{s_1}\left(H_{UC} - \frac{A_{warp}p_{warp}}{10\Gamma_{warp}}\right)^2 \frac{\Gamma_{weft}}{A_{weft}}, \end{aligned} \tag{37}$$

Following the same reasoning as above, scaling coefficient for the warp tow density is obtained as

$$s_{warp} = \frac{\sqrt{s_1}}{s_2}. \tag{38}$$

Substituted into Eq. (36), it produces expression of the scaling factor for H_{UC} as

$$s_H = s_{warp}s_2 = \frac{\sqrt{s_1}}{s_2}s_2 = \sqrt{s_1}. \tag{39}$$

Finally, applying scaling to term Q and making use of scaling factors (38) and (39) yields

$$Q^S = \left(\frac{1}{\sqrt{s_1}s_{weft}} \frac{\Gamma_{weft}}{\Gamma_{warp}} \frac{\left(10\Gamma_{warp}H_{UC} - A_{warp}p_{warp}\right)}{A_{weft}p_{weft}} - 1\right) \frac{1}{\gamma_{weft}}, \tag{40}$$

from which, to maintain $Q^S = Q$ as in Eq. (33),

$$s_{weft} = s_1^{-\frac{1}{2}} \tag{41}$$

should be satisfied.

As a result, scaling factors for the tow densities have been expressed in terms of the scaling factors for tow cross-sectional areas as follows:

$$s_{warp} = \sqrt{s_1}s_2^{-1}, \quad s_{weft} = 1/\sqrt{s_1} \quad \text{and} \quad s_H = \sqrt{s_1}. \tag{42}$$

Scaling the woven architecture according to the rule (42) does not change terms B, C and Q and therefore does not change the KPoWs. Effectively, scaling produces equivalent weave configurations that can have substantially different geometric constructions but identical KPoWs.

3.3. Uniform scaling as a special case

The scaling scheme (42) defines scaling in a general sense, where values of scaling factors associated with different geometric features of the weave can also be different. Consider a special case where the tow sizes are scaled by the same factor, i.e. $s_1 = s_2 = s$. The scaling factors for tow densities become

$$s_{weft} = s_{warp} = 1/\sqrt{s} \quad \text{and} \quad s_H = \sqrt{s}. \tag{43}$$

To facilitate the interpretation of this scaling rule, it is convenient to replace the heigh of the unit cell H_{UC}, which, as has been explained earlier, reflects the density of the tow packing in the thickness direction, with its inverse,

$$p_T = \frac{1}{H_{UC}}, \tag{44}$$

where parameter p_T will be referred to as the density of unit cells through the thickness of the composite. This parameter is expressed in the same units as the two other tow densities, i.e. inverse of length. Scaling factor for this property will naturally become

$$s_T = \frac{1}{s_H}, \tag{45}$$

in which case the scaling factors for tow densities as given by Eq. (43) become identical, namely

$$s_{weft} = s_{warp} = s_T = 1/\sqrt{s}. \tag{46}$$

This signifies that when the weft and the warp tow cross-sections are changed simultaneously by the same factor, the tow densities change by the same factor. Note that the form of the scaling factors reflects the nature of the parameters they are scaling. Specifically, if tow cross-sectional areas that have units of length squared, L^2, are scaled by a factor of s, the tow densities having units of L^{-1}, are scaled by a factor of $s^{-\frac{1}{2}}$. In other words, the linear dimensions are scaled proportionally, while quadratic ones are scaled by the same factor to power two. This type of scaling of the woven geometry will be referred to as the uniform scaling, while scaling cases where $s_1 \neq s_2$ will be referred to as the non-uniform scaling.

3.4. Verification of the scaling procedure

To verify the scaling method derived in the previous section, it can be shown numerically that the KPoWs do indeed stay constant after the controllable parameters are scaled.

To do so, the MATLAB script for calculating the KPoWs has been supplemented with scaling rules given by Eqs. (29) and (42) [24]. It required only a minor modification of the input by allowing the input of two scaling factor, s_1 and s_2, and by multiplying the input tow densities by their respective factors (42). Therefore, to scale a composite configuration, the user only needs to specify the values of s_1 and s_2, and the tow densities will be scaled automatically within the script. The reference (unscaled) values of tow densities can be also reproduced simply by setting $s_1 = s_2 = 1$.

The interlocking angle and the tow ratio associated with 10 reference composite configurations from Table 1 have been plotted in Fig. 4 in black as functions of three tow densities. This presentation adheres to

the same format as has been utilised in Ref. [20]. Consider data corresponding to tow density variation scheme denoted as 'Scheme 2' as an example. In this scheme, two varying tow densities are p_{weft} and H_{UC}. The interlocking angles and tow ratios obtained following this variation scheme are shown as hollow black squares in Fig. 4(a) and (d), respectively, where they are plotted as functions of the weft tow density, both showing the tendency to increase with the latter. In Fig. 4(c) and (f), the same values of respective KPoWs are plotted as functions of H_{UC}. The KPoWs corresponding to the other two tow density variation schemes are plotted against their respective varying tow densities in the same way. Note that third KPoW, the global fibre volume fraction has not been shown as it was kept constant at $V_{f.global} = 0.55$ in all cases.

Both types of scaling, the uniform and non-uniform, were put to the test. For the former, cross-sectional areas in both types of the tows were halved relative to the 'Reference' configurations by setting $s_1 = s_2 = 0.5$, which is equivalent to reducing the fibre count in the warp and the weft tows to 6K. This represents a case of a uniform scaling as was described in subsection 3.3 hence the scaled composite configurations associated with this scaling will be referred to as 'Uniform' ones. The KPoWs corresponding to 'Uniform' configurations have been plotted in Fig. 4 in purple.

Two cases of non-uniform scaling were considered: one where the weft tow cross-sectional area was halved that corresponds to $s_1 = 0.5$ and $s_2 = 1$, and another where the warp tow area was halved, $s_1 = 1$ and $s_2 = 0.5$. The respective scaled configurations have been referred to for brevity as 'Half weft' and 'Half warp'. The KPoWs for the former are plotted in Fig. 4 in orange and for the latter in blue.

Comparing the KPoWs obtained for scaled configurations with those corresponding to the reference ones in Fig. 4(a)–(c), it is obvious that the values of the KPoWs are not affected by scaling. For example, considering the benchmark configurations from all scaling groups, it is easy to see that the values of the respective KPoWs, marked as circles with red boundary, are the same for all of them. The unit cells corresponding to benchmark configurations are shown in Fig. 4(g). Qualitative changes in the UC geometry due to scaling can be summarised as follows:

a) Uniform scaling where cross-sectional areas were reduced leads to simultaneous increase in all three tow densities according to scaling rule (46), hence reduction of the unit cell in all three dimensions.
b) Unit cell corresponding to 'Half warp' scaling case has the same height and length and is half the width of its 'Reference' counterpart. This is consistent with the scaling rule (42), which indicates that the only tow density affected by the warp scaling is p_{warp}. This is the reason why the plots showing the KPoWs as functions of p_{weft} and H_{UC} (Fig. 4(a)–(d) and Fig. 4(c)–(f), respectively) overlap for 'Half warp' and 'Reference' cases.
c) Unit cell corresponding to 'Half weft' scaling case has the same height and length and is double the width of its counterpart obtained through the uniform scaling. Furthermore, uniformly scaled configuration can be recovered from 'Half weft' one simply by applying the non-uniform scaling to the latter that would halve the cross-sectional area warp tow. Effectively, two non-uniform scaling can be applied sequentially in the arbitrary order to deliver a configuration obtained through the uniform scaling. Using mathematical terminology, scaling procedure is commutative in a sense that it does not matter in what order scaling is applied, as long as the final tow sizes are the same.

The results in Fig. 4 also signify that the controllable properties (tow cross-sectional areas) are decoupled from the controllable parameters (tow densities) in a sense that qualitatively, the trends in variation of the KPoWs relative to tow densities are reproduced irrespective of the tow sizes. This offers additional support to the design method [20] that was developed while keeping the tow cross-sectional areas fixed.

Table 2
Properties of the constituent materials [20].

ACTECH 1304 epoxy resin		TZ800H carbon fibre tows		
			weft	warp
E, GPa	3.53 [28]	Intra-tow fibre volume fraction, %	72(76)	75(82)
ν	0.35	E_1, GPa	224.01	241.42
		$E_2 = E_3$, GPa	10.12	11.11
		$\nu_{12} = \nu_{13}$	0.295	0.291
		ν_{23}	0.405	0.393
		$G_{12} = G_{13}$, GPa	6.04	7.406
		G_{23}, GPa	3.60	3.987

4. Mechanical performance of the equivalent configurations of composites

For effective use of scaling in design, it is essential to understand how scaling affects the effective elastic properties; in other words, how different or similar are the effective elastic properties delivered by equivalent composite configurations. To compare the mechanical responses of composites having equivalent configurations of reinforcement, systematic characterisation exercises have been carried out. In Ref. [20], woven composites having configurations as specified in Table 1 have been characterised. The results from that characterisation exercise will be used in the present paper as a reference case and will be compared with the effective properties obtained for configurations produced applying three scaling types as were defined in subsection 3.4.

4.1. Unit cell model and input

To carry out the material characterisation, the unit cell modelling was employed. Use of unit cells that requires idealisation of the internal architecture has been explained and justified in Ref. [20]. Effectively, it strikes a balance between accuracy of predictions they deliver and practicality of their implementation and use in design exercises.

The parametrised unit cell for layer-to-layer angle interlock composites has been established in Ref. [21], where the expressions of the boundary conditions for this unit cell have been provided. The boundary conditions related the displacements on the opposite sides of the unit cell; they were derived following basic principles of deformation kinematics and making proper use of the translational symmetries, thus ensuring the mechanical consistency of formulation. Two types of translations were involved in definition of the unit cell: combination of two orthogonal translations over the cross-section of the weave and a translation in-plane of the weave non-orthogonal to the other two. As was elaborated in Ref. [21], use of such translations allows to reduce the size of the unit cell, thus making it more computational efficient as compared to unit cells defined based on use of orthogonal translations alone. The boundary conditions explicitly involved the six strains at the upper length scale considered as six independent degrees of freedom, which facilitates material characterisation procedure.

The theoretical formulation of the unit cell, its implementation as an FE model and post-processing of the results follows well-established procedures that have been reported multiple times [25,26], with the most comprehensive account being given in Ref. [27], and are therefore not repeated here. From the user's perspective, the material characterisation is carried out in a fully automated manner, because all the associated procedures have been implemented as a designated Python script. The formulation was brought closer to practical applications by expressing the input in terms of controllable parameters in Ref. [22], where he model has extensively been validated against the experimental data.

The same properties of constituents as were employed in Ref. [20] were used in all characterisation cases. For ease of reference, properties of the matrix and the tows are summarised in Table 2. The effective properties of the tows were obtained through unit cell-based

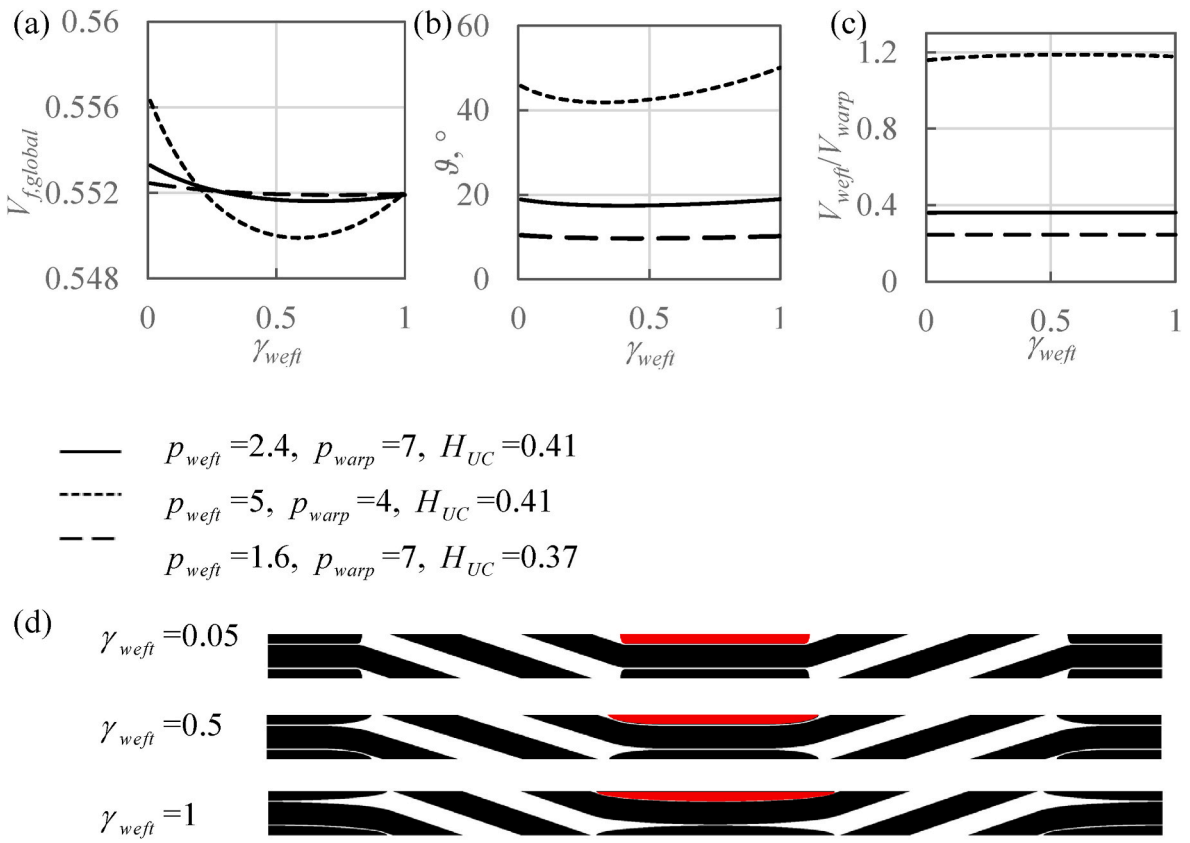

Fig. 5. KPoWs as functions of γ_{weft}: (a) global fibre volume fraction; (b) interlocking angle and (c) tow ratio. Plot (g) - geometries of a UCs representing a benchmark configuration at three different γ_{weft}

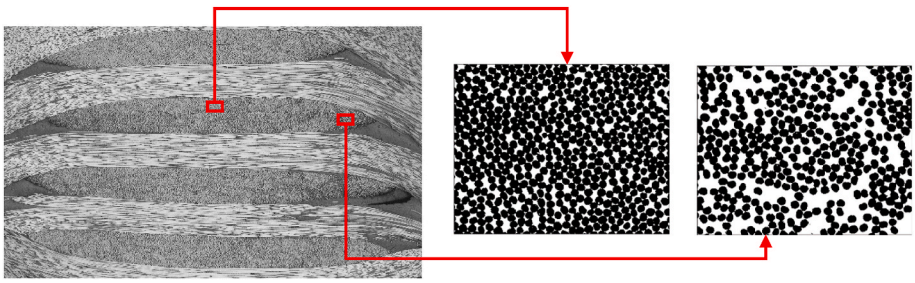

Fig. 6. Typical fibre distribution over the weft tow cross-section in TZ800H composite as characterised in [22].

computational material characterisation where the tows are treated as unidirectional composites at a micro-scale. When conducting characterisation, scaled values of intra-tow fibre volume fractions, as given in brackets in Table 2, were used, reasons for which are explained in Ref. [22], where intra-tow volume fraction scaling procedures are also elaborated.

The controllable parameters associated with the tows were defined in subsection 2.2, along with values of parameters γ_{warp} and γ_{weft} as defined by Eq. (3). These were introduced in Ref. [21] as geometric parameters of tow cross-section, yet unlike other geometric parameters, they have not been expressed in terms of controllable parameters in subsection 2.1. This is because the role of γ is to offer more flexibility in tow cross-section idealisation; in some sense, it is an optional parameter. Special case of $\gamma = 1$ reproduces the elliptical profile, while at values close to zero nearly rectangular cross-section is reproduced, and these two are some of the most common cross-section shapes in idealised models of woven composites [29]. Fixing the value of γ effectively puts restriction on the shape of the cross-section profile.

In the present paper, same values of γ as were employed in previous works [20,22] have been used, $\gamma_{warp} = 0.05$ and $\gamma_{weft} = 0.5$. The justification for the former was to ensure that the warp two cross-section profile stays nearly rectangular, which is a common observation [30]. The definition of value of γ_{weft}, on the other hand, have been left somewhat loose, and the justification is offered below.

Sensitivity of KPoWs to choice of γ_{weft} has been studied by plotting them against γ_{weft} in Fig. 5, while keeping all other parameters fixed. Three composite configurations from Table 1 were considered, a benchmark one, and two representing the cases of high interlocking angle and high tow ratio, and low interlocking angle and low tow ratio, respectively. The most affected KPoW was the interlocking angle, for which the maximum and the minimum in the most extreme case were nearly 10° apart, as can be seen in Fig. 5(b). This was to be expected, because of all geometric parameters (4)–(8), γ_{weft} is involved in definition of width of the weft tow cross-section (7) and, consequently, the distance (8) between the adjacent weft tows, and relative variation of the two inevitably changes the interlocking angle. Interestingly, the

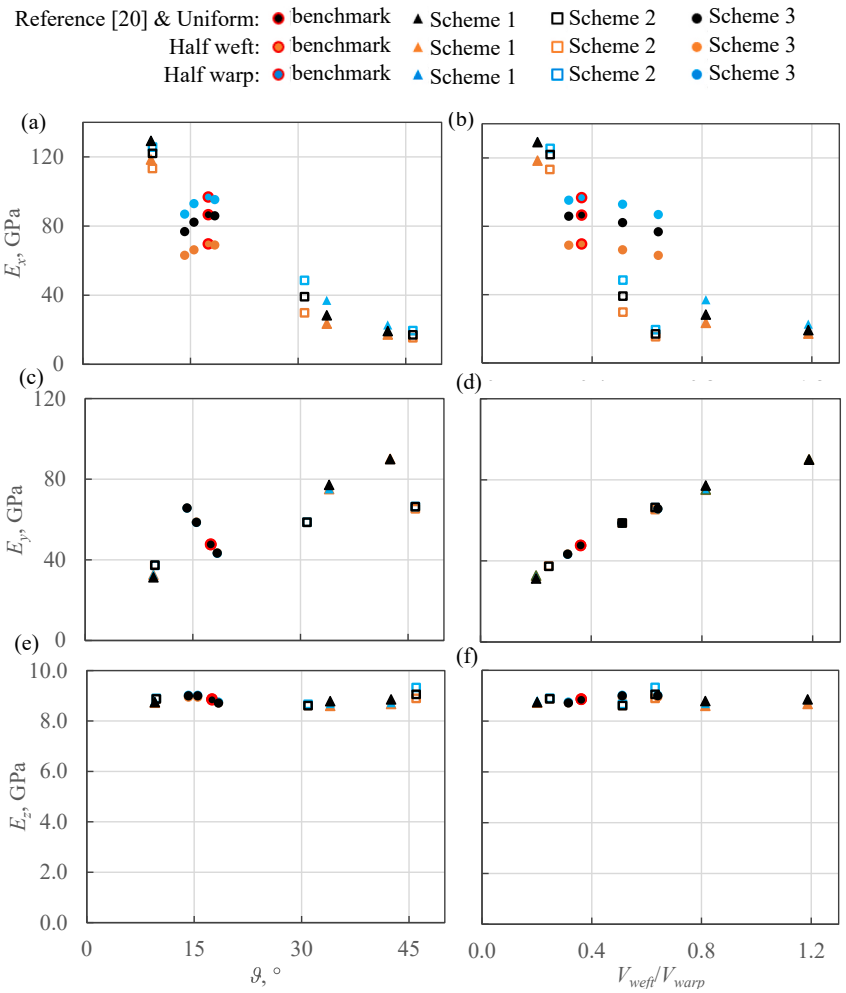

Fig. 7. Effective elastic moduli as functions of the interlocking angle (plots (a),(c) and (e)) and tow ratio (plots (b), (d) and (f)).

other two KPoWs, the global fibre volume fraction and tow ratio, as shown in Fig. 5(a) and (c), show little sensitivity to γ_{weft}, even though interlocking angle is involved in their definitions. The results in Fig. 5 conclude that the KPoWs show little sensitivity to γ_{weft}.

However, there is a practical consideration of why values of γ_{weft} should not be too close to unity, which is its maximum value. Consider the weft cross-section in Fig. 5(d) corresponding to different values of γ_{weft}. Since the weft width increases monotonically with γ_{weft}, as is implied by Eq. (7), the elliptical cross-section would be the widest. Since the area of the weft tow cross-section kept is fixed, the widening of the tow profile is accompanied by the overall reduction in cross-section thickness. As the result, the pointy appearance of the tips of weft tows is the most pronounced in elliptical cross-section compared to cross-section profile obtained at γ_{weft} <1.

Considering the micrograph in Fig. 6 showing typical cross-section view of the weave, pointy tips can also be observed in the weft cross-section. Examining different parts of the weft tow cross-section in Fig. 6, it was found that the fibre packing becomes looser towards the sides of the weft cross-sections. In such regions, the fibre volume fraction can be as low as ~45 %, as opposed to ~70 % in the centre of the tow. This kind of non-uniformity of fibre distribution over the tow cross-section have been previously documented for 2D weaves [31,32]. It can have significant implications on modelling, because due to lower fibre volume fraction, one should expect a reduced material performance in such regions. There is no reliable and robust method for representing gradual reduction of fibre volume fraction in computational models, and in many analyses, including the present one, uniform fibre volume fraction is assumed that corresponds to the tightest packing of the fibres in the tow. Having high stiffness, the pointy tips of the weft tow with elliptical cross-section would act as stress concentrators, which can have a profound difference in strength characterisation exercises. While the present study addresses exclusively the elastic characterisation, maintaining reasonable representation of the tows would be a good practice. To alleviate the adverse effect from the exaggerated stress concentration at the tips of weft cross-sections, γ_{weft} <1 should be used. While this would not bring down the material properties hear the tips of the weft tows hence would not reduce the property mismatch between the tows and the adjacent matrix, it would produce a more rounded appearance of the tips of the tow cross-section, alleviating stress concentrations.

4.2. *Influence of scaling on predictions of the effective elastic properties*

Trends in variation of the effective elastic properties relative to KPoWs for the 'Reference' configurations have been established and discussed in detail in Ref. [20]. To facilitate referencing and comparisons, effective elastic and shear moduli reported in Ref. [20] for the 'Reference' configurations have been plotted in black against the interlocking angle and the tow ratio in Figs. 7 and 8, respectively. The indices for the effective properties are the same as the weave coordinate notations shown in Fig. 1, namely, *x*, *y* and *z* refer to the warp, weft and through-the thickness directions, respectively. Different types of

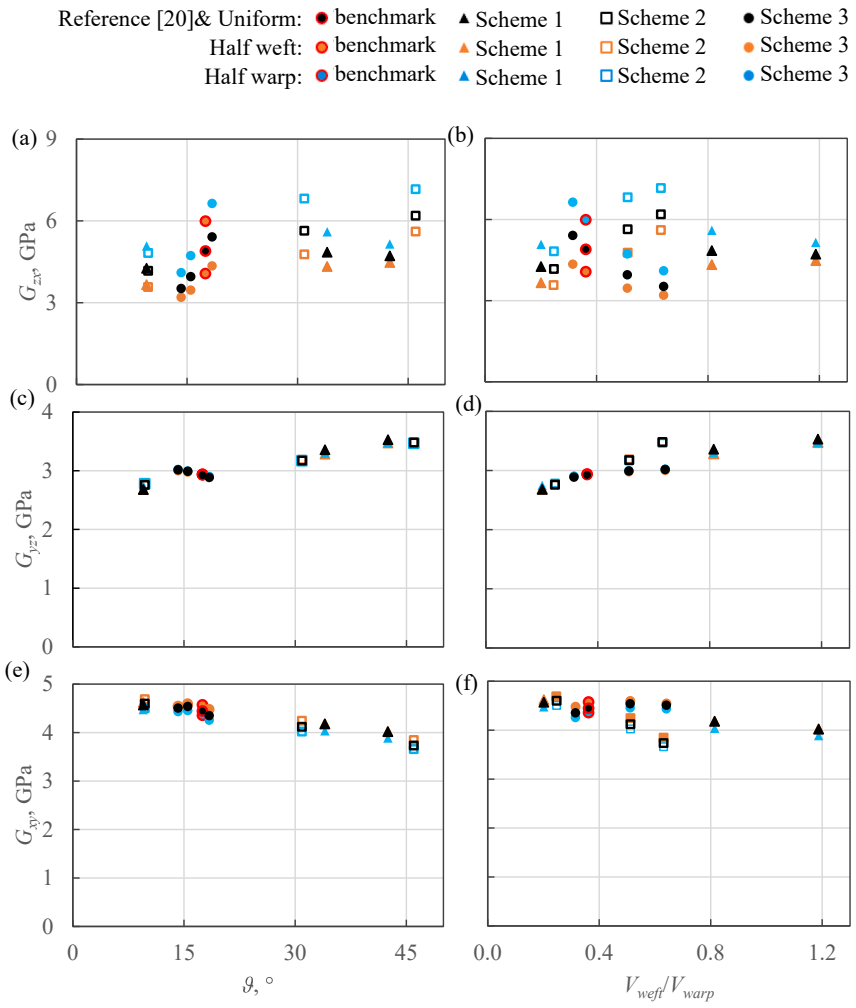

Fig. 8. Effective shear moduli as functions of the interlocking angle (plots (a),(c) and (e)) and tow ratio (plots (b), (d) and (f)).

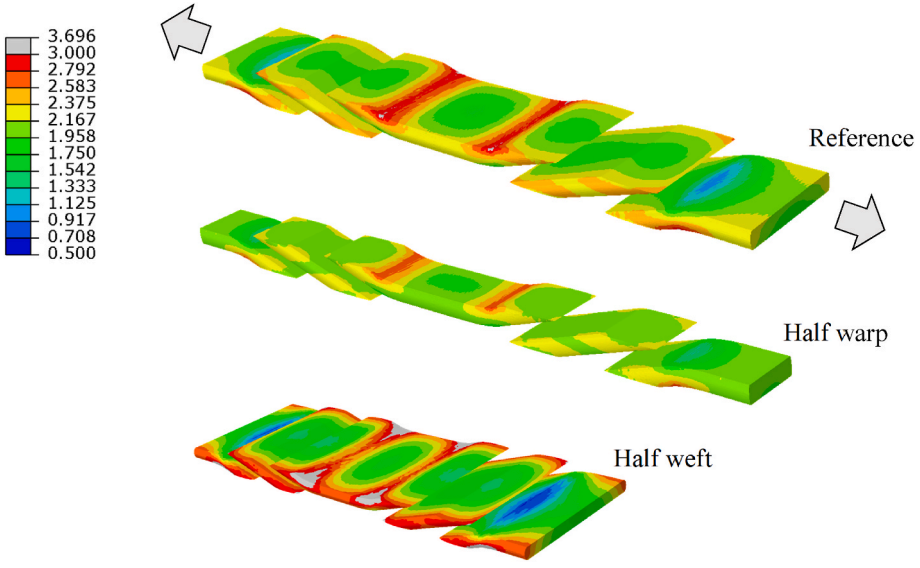

Fig. 9. Contours of the longitudinal stress (stress σ_{11} in local material coordinate system) over the warp tows in the reference and two scaled benchmark configurations.

symbols refer to respective tow density variation schemes in Table 1, same as in Fig. 4.

These have been topped up with characterisation results corresponding to scaled configurations, 10 for each scaling scheme. Their effective elastic and shear moduli have also been plotted against the interlocking angle and the tow ratio in Figs. 7 and 8, respectively. For consistency of presentation, the same colour coding has been retained for the effective properties corresponding to the reference and three scaled groups of the composites as has been introduced for their KPoWs in Fig. 4. Specifically, the effective properties for the reference configurations are plotted in black, those for 'Half weft' configuration are highlighted in orange and the effective properties for 'Half warp' configurations are in blue. Note that the effective properties corresponding to 'Uniform' group share the same black colour as their 'Reference' counterparts. This is because the effective properties in 'Uniform' group identically reproduce those in the 'Reference' group, discounting small numerical errors. This signifies that the uniform scaling, as described in subsection 3.3, represents the method of scaling the geometry that keeps the effective elastic properties the same. Since the uniform scaling factor can be arbitrary, the implications of this are that multiple 3D woven composite configurations can exist, related through the uniform scaling, that would have identical effective elastic properties.

Considering the non-uniform geometry scaling, the effective properties associated the reference configurations have also been reproduced identically in scaled composite configurations with the exception of the warp effective elastic modulus E_x in Fig. 7(a) and (b) and the effective shear stiffness G_{zx} in Fig. 8(a) and (b). For these two, the values corresponding to 'Half weft' scaling scheme are consistently lower than the reference ones, while the values associated with the 'Half warp' scheme are always higher than the reference ones. The reasons why the non-uniform scaling causes mismatch in the effective properties associated with the warp direction can be explained by scrutinising the mechanical behaviour of the woven reinforcement.

Without loss of generality, consider the benchmark configuration from the 'Reference' set and its scaled counterparts. The contours of the stress over the warp tow for all three composite configurations are shown in Fig. 9. The stress is in the fibre direction and the tensile load is applied along the warp direction. Under this type of load, the curved warp tow shows tendency to straightening, the effect of which can be clearly seen in the curved regions of the warp tows. Specifically, localised regions of high and low stress are apparent at the top and bottom surfaces of the warp tows in such regions. Qualitatively, such stress distribution is typical in beam bending problems, when one of the surfaces of the beam is under tension while the opposite one is under compression. For the warp tows in the unit cell, bending-like stress state occurs due to straightening of its curved part under loading in the warp direction; this is not a classical beam bending problem and stresses on the opposite faces of the curved part of the warp tow are of the same sense, but one is significantly larger than the other. Relative to the reference configuration, this effect is less pronounced in the 'Half warp' configuration and is far more apparent in the 'Half weft' configuration.

Considering classical case of beam bending, the resistance to bending is largely controlled by the second moment of area of beam cross-section. For two beams having equal cross-sectional areas, one with cross-section of higher height to width ratio will outperform another in terms of resistance to bending, as it would have larger second moment of area. Considering shapes of cross-sections of the warp tows in Fig. 4(g), it is easy to see that the aspect ratio of the warp tow cross-section in 'Half weft' composite configuration is smaller than the reference one, while the cross-section aspect ratio of the warp tow in 'Half warp' configuration is larger than the reference one. Relating these observations to the results in Fig. 9, an association between the aspect ratio of cross-section and the resistance to straightening under tension in the warp tows can be established. Since load bearing under warp tension is mostly carried out by the warp tows, the less it deforms, the larger will be the warp effective stiffness of the material represented by the unit cell.

It is worth noting that on their own, the second moments of area of the warp tow cross-sections do not provide indication of how effective the warp tows are in resisting the straightening. Indeed, the uniform scaling can deliver numerous composite configurations of very different warp cross-section areas that would naturally have very different second moments of area. However, the aspect ratios of the warp cross-sections will be identical in all such cases and all such configurations will deliver identical effective elastic properties. Effectively, scaling changes the size and dimensions of the unit cell. The change in unit cell size on its own does not affect the effective elastic behaviour, if the dimensions change proportionally, as in the case of uniform scaling, because the unit cell represents infinite material. At the same time, when the non-uniform scaling is applied, the inner dimensions of the weave change to a different extent, which modifies the stress state within the tows as illustrated in Fig. 9 and, as a result, it influences the effective elastic properties associated with the warp direction.

5. Application of scaling in design of 3D woven composites

5.1. Scaling as means of post-processing in design

There are two main consequences of the scaling procedure as far as the composites design is concerned. Firstly, it verifies that the KPoWs do indeed provide sufficient representation of the woven geometry, at least as far as the elastic material characterisation is concerned. It was shown in Ref. [20] that the effective elastic properties follow distinctive trends relative to KPoWs, where the KPoWs were considered as functions of tow densities, while the tow sizes were kept constant. The present research has shown the scaling does not affect these trends; furthermore, it preserves the values of the effective elastic properties with the exception of cases of non-uniform scaling, when values of two elastic properties are systematically higher or lower than the reference ones, the reasons for which were explained in subsection 4.2.

The second major outcome is that the weave scaling procedure conclusively defines the significance and role of the tow sizes in composites design. There is a general perception that the weft tow sizes control the weft properties [33], while there exists an inverse relationship between the interlocking angle and the elastic modulus and strength in the direction of undulating warp tows [2]. However, it was shown in Ref. [20] that the two, in fact, cannot be varied independently and that both in-plane elastic moduli can be modified by varying only the tow densities. Having identified role of scaling as means of varying the geometry and the size of the unit cell representing the woven composite while retaining the same effective elastic behaviour, the number of the designable parameters in design exercises can effectively be reduced to three, namely, the weft, warp and through-the-thickness tow densities. The tow sizes can be chosen upfront, rather randomly, while the tow densities will be varied according to the tow density variation schemes until the desired effective elastic properties are obtained. If the resultant configuration is not practical in terms of the manufacturing, scaling is applied. Additionally, there may be practical restrictions on selection of tow sizes, since the standard sizes as avalable from suppliers are typically restricted to a very few options, e.g. 6K and 12K. If the required tow sizes are not available, there is no need to re-design the material, or to resort to tow adding/splitting; scaling will maintain the effective elastic properties while accommodating different sizes of the tows. Effectively, scaling can be viewed as means of 'post-processing' the design to make it practical.

It should be noted that not recognising different roles of tow densities and tow cross-sectional areas in design may lead to misinterpretation of the results of design exercises. Specifically, in Ref. [9], comparison of the effective properties corresponding to four 3D woven composite configurations was carried out, where both the tow sizes (hence cross-sectional areas) and the tow densities were changed simultaneously, yet any changes in values of the effective elastic properties were attributed exclusively to different tow sizes, while the influence of tow densities

Table 3
Controllable parameters and KPoWs for three scaled composite configurations.

Configuration	Tow sizes		Tow densities			Key properties of the weave		
	N_{weft}	N_{warp}	p_{weft}, cm^{-1}	p_{warp}, cm^{-1}	H_{UC}, mm	ϑ °	$\frac{V_{weft}}{V_{warp}}$	$V_{f\text{-}global}$
Original [22]	12K	12K	2.9	7	0.41	24.8	0.429	0.59
Scaled (Eq. (42))	6K	6K	4.1	9.9	0.29	24.8	0.429	0.59
Guessed [34]	6K	6K	4.3	10	0.33	24.0	0.442	0.53

Table 4
Effective properties for three scaled composite configurations.

Configuration	E_x, GPa	E_y, GPa	E_z, GPa	G_{zx}, GPa	G_{xy}, GPa	G_{yz}, GPa
Original	65.40	56.11	9.16	5.33	4.58	3.17
Scaled	65.40	56.11	9.16	5.33	4.58	3.17
Guessed	55.82	51.87	8.48	5.33	4.13	2.97

was not even contemplated. Similarly, the parametric studies in Ref. [8] aimed to reveal the influence of tow densities on the effective elastic and strength properties. However, the cross-sectional areas in this study were considered as functions of the weft and warp tow densities, therefore the latter were also varying between different models. The present paper conclusively establishes that both groups of controllable parameters, namely, the tow densities and the tow sizes, play equally important parts in variation of the effective elastic properties and none of them should be disregarded.

This design method offers scope for extension to other types of 3D woven composites. From practical perspective, most of the designable parameters should be the same for different types of 3D weaves, while additional research may be required to identify the key properties of the weave that are associated with trends in variation of the effective elastic properties in other types of 3D woven composites.

Equally important application of scaling could be in design exercises involving damage and strength characterisation. These mechanical behaviours are sensitive to local geometric features of the woven reinforcement where stress concentrations can build up. Scaling could help maintain the same initial elastic performance while modifying the undesirable geometric features to alleviate potential stress concentrations. The analogy can be drawn to ultra-thin laminates which, due to substantially reduced size of a ply, deliver higher resistance to damage and failure. Design exercises involving material strength characterisation may also require definition of geometric characteristics of the weave that are associated with localised stress distributions, such as the warp tow cross-section aspect ratio mentioned in subsection 4.2. The design method as established here offers means for conducting systematic studies that could help identifying such characteristics.

5.2. Intuitive vs precise scaling

As a demonstration of application of scaling capability, consider two TZ800H woven composites with controllable parameters specified Table 3, referred to as ‘Original’ configuration and ‘Guessed’ configuration. As can be seen, the sizes of the tows, 6K, in the latter are half those in the former. The ‘Original’ configuration was previously characterised in Ref. [22], where calculated in-plane effective properties were also compared with the measured ones, while the motivation for producing ‘Guessed’ configuration in Ref. [34] was to assess whether composites having significantly different tow sizes but similar KPoWs would have similar mechanical performance. In absence of design methodology at the time, the only design means available have been the computational material characterisation tool and intuition. As can be seen in Table 3, the KPoWs in the two configurations turned out to be similar, though not identical. However, considering values of the effective properties for this two configurations as listed in Table 4, it is easy to see that the values of effective warp and the weft elastic moduli in ‘Guessed’ configuration are noticeably lower than the values of their ‘Original’ counterparts. This is consistent with discrepancy in global fibre volume fractions, which is lower in ‘Guessed’ configuration, and this naturally has a knock-on effect on the effective elastic properties. Comparing ‘Guessed’ values of tow densities with those obtained by applying scaling rule (42) (these correspond to ‘Scaled’ configuration in Table 3), it can be seen that all three followed correct variation trends. Still, achieving the exact scaled down geometry that would deliver the same mechanical performance through trial-and-error would have required a lot of effort. On the other hand, scaling rule (42) delivers scaled configuration in a matter of seconds, which makes it an extremely efficient tool in composites design.

6. Conclusions

Problem of geometric scaling in 3D layer-to-layer angle interlock woven composites has been raised and resolved for the first time. Scaling was shown to be a special case of variation of the reinforcement architectures for which the effective elastic properties of composites based on such reinforcement are identical, in case of uniform scaling, or show systematic deviation from the reference values in two properties associated with the warp direction for non-uniform scaling. Existence of such configurations has not been discussed, let alone been proven to date, as most of the efforts in defining the association between the internal construction and the mechanical performance have been directed at identified trends in variation of the properties rather than the conditions when they would remain unchanged.

Scaling was found to be controlled by two designable properties, the cross-sectional areas of the weft and warp tows. This disproves a common perception that in 3D woven composites the tow sizes are the appropriate means of varying the in-plane effective properties. Since the uniform scaling does not bring about any change in the effective properties, obviously, even a significant change in tow sizes would not have any effect on the properties in scaled composite configurations.

It was previously established in Ref. [20] that designable parameters that can be used most effectively for varying the elastic properties of 3D woven composites are the tow densities. Present work defines the geometry variation rules that delivers exactly the opposite, namely, constancy of the effective properties when the geometry changes rather than trends in their variation. Combined, these two considerations provide a robust design method for 3D layer-to-layer angle interlock woven composites, where roles of two groups of the designable parameters are clearly defined. Specifically, the desired mechanical performance is achieved through systematic variation of the tow densities, while scaling is applied as a post-processing of design of woven architecture to ensure its practicality, if necessary.

Complexity of internal architectures and lack of methods for their design are common not only of 3D woven composites, but for advanced materials of complex internal architecture in general. The awareness of the concept of scaling as a special type of internal architecture variation that is raised by the present paper can be instrumental in development of the analysis and design methods for many types of advanced materials.

CRediT authorship contribution statement

Elena Sitnikova: Writing – review & editing, Writing – original draft, Visualization, Validation, Methodology, Investigation, Conceptualization. **Shuguang Li:** Writing – review & editing, Conceptualization.

Declaration of competing interest

The authors declare that they have no known competing financial interests or personal relationships that could have appeared to influence the work reported in this paper.

Acknowledgements

The authors acknowledge assistance of Dr. Shuang Qin, postdoctoral researcher at the Institute of Mechanics, Chinese Academy of Sciences, Beijing, China and Dr. Mingming Xu, Assistant Professor at Beijing Institute of Technology, Zhuhai campus, on producing and processing the micrographs of tow cross-sections.

Appendix A. Supplementary data

Supplementary data to this article can be found online at https://doi.org/10.1016/j.compscitech.2026.111517.

Data availability

The Matlab script was shared at Mendeley Data repository and it is cited in the paper

References

[1] S. Dai, P.R. Cunningham, S. Marshall, C. Silva, Influence of fibre architecture on the tensile, compressive and flexural behaviour of 3D woven composites, Compos. Appl. Sci. Manuf. 69 (2015) 195–207.
[2] E. Archer, S. Buchanan, A. McIlhagger, J. Quinn, The effect of 3D weaving and consolidation on carbon fiber tows, fabrics, and composites, J. Reinforc. Plast. Compos. 29 (20) (2010) 3162–3170.
[3] M. Dahale, G. Neale, R. Lupicini, L. Cascone, C. McGarrigle, J. Kelly, E. Archer, E. Harkin-Jones, A. McIlhagger, Effect of weave parameters on the mechanical properties of 3D woven glass composites, Compos. Struct. 223 (2019) 110947.
[4] R. Umer, H. Alhussein, J. Zhou, W. Cantwell, The mechanical properties of 3D woven composites, J. Compos. Mater. 51 (12) (2017) 1703–1716.
[5] Y. Zhang, J. Feng, J. Yan, Q. Guo, Z. Sun, D. Zhang, J. Guo, L. An, X. Wu, L. Chen, Effect of weave pattern on the low-velocity impact properties of 3D woven composites, Thin-Walled Struct. 209 (2025) 112969.
[6] S. Buchanan, A. Grigorash, E. Archer, A. McIlhagger, J. Quinn, G. Stewart, Analytical elastic stiffness model for 3D woven orthogonal interlock composites, Compos. Sci. Technol. 70 (11) (2010) 1597–1604.
[7] Z-g Li, D-s Li, H. Zhu, Z-x Guo, L. Jiang, Mechanical properties prediction of 3D angle-interlock woven composites by finite element modeling method, Mater. Today Commun. 22 (2020) 100769.
[8] Y-x Sun, T-l Yao, X. Yang, D-s Li, L. Jiang, H-m Zuo, S.V. Lomov, F. Desplentere, Parametric modeling on warp and weft tensile strength prediction and progressive damage evolution of 3D angle-interlock woven composites, Compos. Struct. 362 (2025) 119072.
[9] Z. Wang, C. Zhao, Z. Yang, K. Wang, G. Dong, M.D. Starostenkov, Multi-scale collaborative prediction of optimal configuration for carbon fiber woven composites based on deep learning neural networks, Compos. Struct. 339 (2024) 118165.
[10] G. Hwang, D.H. Kim, M. Kim, Structure optimization of woven fabric composites for improvement of mechanical properties using a micromechanics model of woven fabric composites and a genetic algorithm, Compos. Adv. Mater. 30 (2021), 26349833211006114.
[11] M. Esmaeeli, M.R. Nami, B. Kazemianfar, Geometric analysis and constrained optimization of woven z-pinned composites for maximization of elastic properties, Compos. Struct. 210 (2019) 553–566.
[12] E. Ghane, M. Fagerström, S.M. Mirkhalaf, A multiscale deep learning model for elastic properties of woven composites, Int. J. Solid Struct. 282 (2023) 112452.
[13] K. Liu, F. Wang, X. Wang, B. Yan, M. Tong, Prediction of elastic properties of 3D orthogonal woven composites by multiscale deep neural network, Mater. Today Commun. 42 (2025) 111221.
[14] D.-J. Kim, G.-W. Kim, J-h Baek, B. Nam, H.-S. Kim, Prediction of stress-strain behavior of carbon fabric woven composites by deep neural network, Compos. Struct. 318 (2023) 117073.
[15] X. Liu, X.-Y. Zhou, B. Liu, C. Gao, Multiscale modeling of woven composites by deep learning neural networks and its application in design optimization, Compos. Struct. 324 (2023) 117553.
[16] A. Koptelov, A. Thompson, S.R. Hallett, B. El Said, A deep learning approach for predicting the architecture of 3D textile fabrics, Mater. Des. 239 (2024) 112803.
[17] Z. Wu, Three-dimensional exact modeling of geometric and mechanical properties of woven composites, Acta Mech. Solida Sin. 22 (5) (2009) 479–486.
[18] A.R. Labanieh, X. Legrand, V. Koncar, D. Soulat, Novel optimization method to estimate the geometrical properties of a multiaxial 3D woven preform, J. Reinforc. Plast. Compos. 32 (10) (2013) 700–712.
[19] Z.-P. Wang, B.N. Cox, S.J. Kuehsamy, M.H. Jhon, O. Sudre, N. Sridhar, G. J. Conduit, A compact yet flexible design space for large-scale nonperiodic 3D woven composites based on a weighted game for generating candidate tow architectures, Comput. Aided Des. 167 (2024) 103637.
[20] E. Sitnikova, M. Xu, W. Kong, S. Hu, S. Li, Design strategy for 3D layer-to-layer angle interlock woven composites, Mater. Des. 247 (2024) 113414.
[21] M. Xu, E. Sitnikova, S. Li, Unification and parameterisation of 2D and 3D weaves and the formulation of a unit cell for composites made of such preforms, Compos. Appl. Sci. Manuf. 133 (2020) 105868.
[22] E. Sitnikova, M. Xu, W. Kong, S. Li, Controllable parameters as the essential components in the analysis, manufacturing and design of 3D woven composites, Compos. Sci. Technol. 230 (2022) 109730.
[23] E. Sitnikova, Calculation of the key properties of the weave, Mendeley Data (2023), https://doi.org/10.17632/tzhjg99wt7.1.
[24] E. Sitnikova, Scaling 3D layer-to-layer angle interlock woven reinforcements, Mendeley Data (2025), https://doi.org/10.17632/pfgyxdvkb4.1.
[25] S. Li, General unit cells for micromechanical analyses of unidirectional composites, Compos. Appl. Sci. Manuf. 32 (6) (2001) 815–826.
[26] S. Li, L.F.C. Jeanmeure, Q. Pan, A composite material characterisation tool: unitcells, J. Eng. Math. 95 (1) (2015) 279–293.
[27] S. Li, E. Sitnikova, Representative Volume Elements and Unit Cells: Concepts, Theory, Applications and Implementation, Elsevier, 2019.
[28] ACTECH 1304 epoxy resin datasheet, AVIC Composite Co., LTD, 2020.
[29] S.V. Lomov, G. Huysmans, Y. Luo, R.S. Parnas, A. Prodromou, I. Verpoest, F. R. Phelan, Textile composites: modelling strategies, Compos. Appl. Sci. Manuf. 32 (10) (2001) 1379–1394.
[30] M. Xu, E. Sitnikova, W. Kong, J. Zhang, S. Hu, S. Li, Characterisation of 3D woven textile composites in presence of minor weft tow undulations and cross-section variations, J. Compos. Mater. 58 (25) (2024) 2671–2691.
[31] H.M. El-Dessouky, C.A. Lawrence, Ultra-lightweight carbon fibre/thermoplastic composite material using spread tow technology, Compos. B Eng. 50 (2013) 91–97.
[32] D.M. Blackketter, D.E. Walrath, A.C. Hansen, Modeling damage in a plain weave fabric-reinforced composite material, J. Compos. Technol. Res. 15 (1993) 136–142.
[33] Z. Liu, J. Ge, K. Liu, M. Li, B. Zhang, H. Wang, J. Huang, J. Liang, High-fidelity modeling of 3D woven composites considering inhomogeneous intra-yarn fiber volume fractions, Compos. Struct. 290 (2022) 115505.
[34] M. Xu, Design of Architecture of 3D Woven Composites for Impact Resistance, University of Nottingham, 2022.